verted to the trihexyl ester with 3 equivalents of *n*-hexanoyl chloride in pyridine (90%). The triester was reacted with *N-t*-BOC-glycine (BOC, butoxycarbonyl), dicyclohexylcarbodiimide (DCC), and 4-dimethylaminopyridine (DMAP) in pyridine, forming the *N-t*-BOC-glycylaminomethane derivative of the triester (68%). Hydrolysis of the ester groups ($K_2CO_3$ in 95% ethanol) (94%), followed by treatment with $CH_3SO_2Cl$ in $CH_2Cl_2$, yielded tris(3-methanesulfonyloxypropyl)-*N-t*-BOC-glycylaminomethane (97%). Reaction of this trimesylate with sodium thiolacetate in MeOH at reflux for 5 hours afforded the trithiolacetate ester (46%) that was converted to **1** after 5 hours at reflux in methanol and HCl (100%). Full details of this preparation will be reported separately.

17. A Nicolet (Madison, WI) 510P FTIR spectrometer equipped with a mercury cadmium telluride (MCT) detector, a Spectra Tech (Stamford, CT) model FT-80 grazing-angle (80°) reflectance accessory, and a Spectra Tech aluminum-wire grid on zinc selenide substrate polarizer.
18. Ellipsometry measurements on the polyalanine layer were highly variable, indicating uneven chain growth. Nonetheless, there was no indication of incorporation of the solvent (acetonitrile) in the layers (the layers were rinsed with ethanol and air dried before analysis). The absorptions of the 24-mer and the polymer layer in Fig. 3A are 0.009 and 0.34, respectively, from which we conclude that the polymer layer consists of approximately 900 alanine units. Each amino acid residue contributes 1.5 Å to the length of the helix, and thus, the polymer layer is 1300 to 1400 Å thick.
19. The IR spectral details of α-helical and β–pleated sheet forms of peptides have been studied in detail: see T. Miyazawa and E. R. Blout, *J. Am. Chem. Soc.* **83**, 712 (1961); D. Muller and H. R. Kricheldorf, *Polym. Bull.* **6**, 101 (1981).
20. The monolayer of **1** on gold is also quite stable and is unchanged after heating at 150°C for 2 days.
21. The procedure for modification of ITO glass was that described in K. Chen, W. B. Caldwell, C. A. Mirkin, *J. Am. Chem. Soc.* **115**, 1193 (1993); R. C. Cieslinski and N. R. Armstrong, *J. Electrochem. Soc.* **127**, 2605 (1980). The surface metal–OH groups are spaced further apart on this and other glass surfaces than are the gold atoms on a gold surface, providing room for the growth of helical polyalanine without the use of trithiol **1**. However, the greater degree of randomness and inhomogeneity of a glass surface compared with that of gold is reflected in a lower degree of order in the polymer grown on the former.
22. This layer need not be as ordered as the first, and we expect that unreacted α-chloroamide residues remain.
23. Supported by the National Science Foundation Small Grant for Exploratory Research DMR-9014026 and the Robert A. Welch Foundation.

5 February 1993, accepted 13 May 1993

---

# Quantification of the Influence of Surface Structure on C–H Bond Activation by Iridium and Platinum

Dale F. Johnson and W. Henry Weinberg*

**The trapping-mediated dissociative chemisorption of ethane on the closest packed Ir(111) surface has been investigated, and the activation energy and preexponential factor of the surface reaction rate coefficient have been measured. These results are compared to those of ethane activation on Pt(111) and on the missing row reconstructed Ir(110)-(1×2) and Pt(110)-(1×2) surfaces, allowing a quantitative determination of the effect surface structure has on the catalytic activation of C–H bonds. In the order Pt(111), Pt(110)-(1×2), Ir(111), and Ir(110)-(1×2), the activation energies for the dissociative chemisorption of ethane are 16.6, 10.5, 10.3, and 5.5 kilocalories per mole, demonstrating that the electronic and geometric effects are of approximately equal importance for ethane activation on these catalysts.**

The catalytic reforming of petroleum naphtha fractions by supported bimetallic platinum and iridium catalysts is a process of great commercial importance in the fuels industry. The objective of reforming is the selective conversion of saturated hydrocarbons into high-octane aromatic components for gasoline. The overall yield of the process, however, is hampered by the competing hydrogenolysis of the feed stream hydrocarbon reactants (*1*). Also of importance in this industry is the catalytic conversion of $C_1$ to $C_4$ alkanes in natural gas into value-added fuel and feedstock chemicals (*2*). The common technological challenge relevant to these processes is the activation of the strong alkane C–H bonds: 105 kcal/mol for methane, 98 kcal/mol for primary bonds, 95 kcal/mol for secondary bonds, and 93 kcal/mol for tertiary bonds (*3*).

On supported catalysts, the metallic component is dispersed as small (10 to 100 Å) particles on high surface area substrates of alumina or silica, for example, in which a large fraction of the metal atoms may be considered as surface atoms (*1*, *4*). The distinct microstructures of these crystallites induce steric and electronic differences among the catalytic sites, with those on the faceted surfaces having relatively lower reactivities than those at the edges and defects. In an effort to go beyond this qualitative description, we have undertaken a quantitative determination of the effect surface structure has on C–H bond activation.

Both platinum and iridium form face-centered-cubic lattice structures, and the four surfaces of interest in this report are Pt(111), Ir(111), Pt(110)-(1×2), and Ir(110)-(1×2). The (111) surfaces are the most stable, closest packed arrangements of surface metal atoms, whereas the (110) surfaces reconstruct into a (1×2) surface unit cell, often referred to as the "missing row" structure (*5*). A measure of the structural sensitivity of these four surfaces toward alkane activation is found in the results of ultrahigh vacuum (UHV) thermal desorption and low-energy electron diffraction studies (*6*–*8*). The threshold temperatures for the thermal activation of alkane C–H bonds were found to be 130 K for Ir(110)-(1×2) and 200 K for Pt(110)-(1×2). Under these UHV conditions, Ir(110)-(1×2) activates all alkanes except methane, Pt(110)-(1×2) activates only $C_4$ and higher alkanes, and Ir(111) and Pt(111) fail to activate saturated hydrocarbons up to $C_7$ and $C_8$, respectively.

Our understanding of the influence of surface geometric and electronic structure on catalysis has been extended considerably by recent studies of the apparent kinetic parameters of C–H bond activation on these four surfaces (*9*–*11*). We report here the results of experiments concerning the activation of $^{13}C$-labeled ethane ($C_2H_6$) on Ir(111), which, when combined with recent studies of this reaction on Pt(111), Pt(110)-(1×2), and Ir(110)-(1×2), quantify the significant influence exerted by surface structure on C–H bond activation. As would be expected, the initial step in the activation of $C_2H_6$ is C–H (and not C–C) bond cleavage (a deuterium kinetic isotope effect was observed on all four surfaces).

The measurements on the Ir(111) surface were carried out in an ion-pumped UHV microreactor (200 liter/s) that has a base pressure of $2 \times 10^{-10}$ torr and a volume of 10 $cm^3$ (*10*, *12*). For the dissociative chemisorption of $C_2H_6$ over the surface temperature range that was used ($450 K < T_s < 1200 K$), the system was operated in a continuous flow mode. With the crystal held at a constant temperature, a $C_2H_6$ pressure of $1.0 \times 10^{-7}$ torr was maintained for a reaction time, $\tau$. The gas temperature, $T_g$, was always equal to the wall temperature (~300 K) because the mean-free path of $C_2H_6$ at this pressure was much greater than the dimensions of the microreactor. We determined the amount of dissociated $C_2H_6$ by titrating the carbonaceous residue on the surface after reaction with excess oxygen, producing exclusively $^{13}C$-labeled $CO_2$ (*13*). By counting mass spectrometrically the amount of $^{13}CO_2$ that was produced, we obtained the total number of $^{13}C$ adatoms on the surface, $N_c$. The reaction conditions and times were such that the fractional coverage of $^{13}C$ adatoms was between 5 and 10% of a monolayer of carbidic carbon. The lower limit ensures

---

Department of Chemical Engineering, University of California, Santa Barbara, CA 93106.

*To whom correspondence should be addressed.

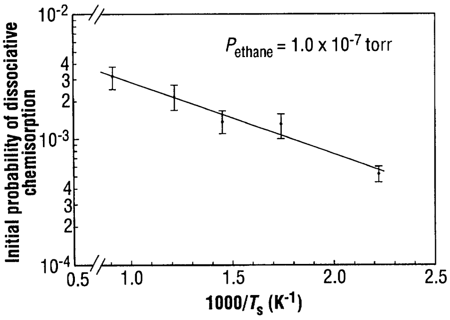

**Fig. 1.** Initial probability of trapping-mediated dissociative chemisorption of $C_2H_6$ on Ir(111) as a function of reciprocal surface temperature. The slope, $-(E_r - E_d)/k_B$, and intercept, $k_r^{(0)}/k_d^{(0)}$, are reported in Table 1. The error bars represent 1 SD in the measured rate at each temperature.

**Table 1.** Rate parameters for the dissociative chemisorption of $C_2H_6$ on Ir(111), Pt(111), Ir(110)-(1×2), and Pt(110)-(1×2). The separately measured value for the desorption rate coefficient was used in evaluating $E_r$ and $k_r^{(0)}$. The quantity $E_r - E_d$ is the activation energy with respect to a gas-phase energy zero, that is, the gas-phase $C_2H_6$ infinitely far from the surface and at rest, whereas $E_r$ is the activation energy of the reaction with respect to the proper reference energy, namely, the bottom of the physically adsorbed well.

| Surface | $E_r - E_d$ (kcal/mol) | $k_d^{(0)}/k_r^{(0)}$ | $E_r$ (kcal/mol) | $k_r^{(0)}$ ($s^{-1}$) | Reference |
|---|---|---|---|---|---|
| Ir(111) | 2.6 ± 0.2 | 100 | 10.3 | $1 \times 10^{11}$ | This work |
| Pt(111) | 8.9 ± 0.8 | 1200 | 16.6 | $8 \times 10^{9}$ | (*9*) |
| Pt(110)-(1×2) | 2.8 ± 0.2 | 200 | 10.5 | $5 \times 10^{10}$ | (*10*) |
| Ir(110)-(1×2) | −2.2 ± 0.2 | 400 | 5.5 | $3 \times 10^{10}$ | (*11*) |

that the results are not dominated by reactivity at surface defects (*14*), whereas the upper limit ensures that the initial rate of the C–H activation reaction has been measured; that is, the rate is approximately characteristic of a clean Ir(111) surface. This enhanced reactivity at steps and defect sites on the surface that we have observed (*14*) verifies that we are actually measuring the (low) reactivity of $C_2H_6$ and not the (high) reactivity of a contaminant hydrocarbon present in the vacuum chamber in low concentrations. At a given $T_s$, the probability of dissociative chemisorption, $P_r(T_s)$, is obtained from

$$P_r(T_s) = \frac{N_c}{2A\tau F} \tag{1}$$

where $A$ is the sample surface area, $F$ is the impingement flux of reactant molecules, and the stoichiometric factor of 2 converts $N_c$ into the number of dissociated $C_2H_6$ molecules.

The study of alkane activation by single-crystalline transition metal surfaces reveals that two fundamentally different reaction mechanisms may be operative: (i) direct dissociation (*11, 15*) and (ii) trapping-mediated, dissociative chemisorption (*16, 17*). Direct dissociation occurs on the time scale of a collision between the gas-phase molecule and the surface ($<10^{-12}$ s), and the rate of this reaction depends primarily on the translational and internal energies of the gas-phase molecule. In trapping-mediated, dissociative chemisorption, the gas-phase molecule is trapped in the potential field of the surface (that is, it is adsorbed molecularly in the case of $C_2H_6$) and it accommodates to the temperature of the surface. The physically adsorbed molecule may then either desorb with a rate coefficient $k_d$ or it may react (dissociate) with a rate coefficient $k_r$. The relative rates of these competing reactions are dependent on $T_s$, provided that the associated activation energies of desorption, $E_d$, and reaction, $E_r$, are not equal. The gas temperature is important only insofar as it affects the probability of trapping into the physically adsorbed state.

For the dissociative chemisorption of physically adsorbed $C_2H_6$, the initial C–H bond cleavage is rate limiting (*6, 7, 18*). The resulting chemisorbed ethyl undergoes further dehydrogenation and ultimately C–C bond cleavage at elevated $T_s$. This reaction sequence may be written as

$$C_2H_{6(g)} \underset{k_d}{\overset{\xi F}{\rightleftarrows}} C_2H_{6(p)} \xrightarrow{k_r}$$

$$C_2H_{5(c)} + H_{(c)} \rightarrow 2C_{(c)} + 3H_{2(g)}$$

where $\xi$ is the probability of trapping $C_2H_6$ into the physically adsorbed well; g, p, and c denote gaseous, physically adsorbed, and chemisorbed states, respectively; and $k_d$ and $k_r$ are the elementary rate coefficients for desorption and reaction and are of the Polanyi-Wigner form, namely,

$$k_i = k_i^{(0)} e^{-E_i/k_B T_s} \tag{2}$$

where $k_B$ is the Boltzmann constant. If $T_s$ is sufficiently high that the fractional coverage of the physically adsorbed $C_2H_6$ is negligibly small, as is the case for the experiments reported here, then a pseudo–steady-state analysis yields the following expression for the probability of $C_2H_6$ activation, which is the ratio of the reaction rate to the impingment rate (*17*):

$$P_r = \frac{\xi k_r}{k_d + k_r} \tag{3}$$

In general, Eq. 3 implies that

$$\frac{\xi}{P_r} - 1 = \frac{k_d}{k_r} \tag{4}$$

and, for the special case of $k_r << k_d$, both Eqs. 3 and 4 reduce to

$$\frac{P_r}{\xi} = \frac{k_r}{k_d} \tag{5}$$

For $C_2H_6$ activation on Ir(111), we have found experimentally that $k_r << k_d$; consequently, a semilogarithmic plot of $P_r$ as a function of $1/T_s$ yields the apparent kinetic parameters of the elementary C–H bond scission reaction. Figure 1 is such an Arrhenius plot for the dissociative chemisorption of $C_2H_6$ on Ir(111). Combining Eqs. 2 and 5 yields

$$\frac{P_r}{\xi} = \frac{k_r^{(0)}}{k_d^{(0)}} e^{-(E_r - E_d)/k_B T_s} \tag{6}$$

from which it is apparent that the slope of the straight line in Fig. 1 is equal to $-(E_r - E_d)/k_B$, and the intercept is equal to $k_r^{(0)}/k_d^{(0)}$.

As on Ir(111), $C_2H_6$ activation on Pt(111) and Pt(110)-(1×2) proceeds with $k_r << k_d$, and the apparent kinetic parameters are obtained just as described above (*9, 10*). On Ir(110)-(1×2), however, the special case of $k_r << k_d$ is inapplicable, and the semilogarithmic plot of the quantity $\xi/P_r - 1$ as a function of $1/T_s$ must be used (*11*). By combining Eqs. 2 and 4, one concludes that the slope of this semilogarithmic plot is equal to $-(E_d - E_r)/k_B$, and the intercept is equal to $k_d^{(0)}/k_r^{(0)}$. Together, the linearity of these constructions and the observed variation of the reaction rate with $T_s$ (at constant $T_g$) confirm that the surface reaction obeys a trapping-mediated mechanism. In constructing Fig. 1 [as well as the figures in (*9–11*)], it was recognized that the trapping probability is only a weak function of $T_s$ (*19*), and it was reasonably assumed that the trapping probability is unity for a Maxwell-Boltzmann energy distribution of $C_2H_6$ at 300 K (*16*).

Table 1 provides the energy differences, $E_r - E_d$, and the ratios of preexponential factors, $k_d^{(0)}/k_r^{(0)}$, for the activation of $C_2H_6$ on all four surfaces. For the atomically flat surfaces of both metals and for the corrugated Pt surface, $E_r - E_d > 0$, implying that for each of these systems there is an activation barrier with respect to the gas-phase energy zero. For the corrugated Ir surface, however, $E_r - E_d < 0$, and this reactive system is unactivated with respect to this gas-phase zero. It is noteworthy that $k_d^{(0)}/k_r^{(0)} > 1$ for all four systems, as would be expected in view of the greater entropy associated with the transition state for desorption relative to the transition state for C–H bond cleavage (*18*). Because the activation energy and preexponential factor for desorption of physically adsorbed $C_2H_6$ are approximately 7.7 kcal/mol and $10^{13}\ s^{-1}$, respectively (*7*), the activation energies, $E_r$, and preexponential factors, $k_r^{(0)}$, for dissociative chemisorption may be evaluated easily (these values are also listed in Table 1).

From these results, the electronic and geometric effects on C–H bond activation of these four surfaces of Pt and Ir can be discussed quantitatively. The $E_r$ values given in Table 1 provide the magnitudes by which the Ir surfaces of a given geometry are more active than the corresponding Pt surfaces and by which the corrugated (110) surfaces of each metal are more reactive than their atomically flat (111) counterparts. By comparing samples of the same crystallographic orientation, we find that the $E_r$ value on Ir is 5.0 to 6.3 kcal/mol lower than that on Pt. For each metal, the corrugated (110)-(1×2) surfaces have $E_r$ values that are 4.8 to 6.1 kcal/mol lower than those of the close-packed (111) surfaces. Consequently, the Pt(110)-(1×2) and Ir(111) surfaces have approximately equal activity toward $C_2H_6$ activation, demonstrating that the difference in geometric structure compensates for the intrinsic electronic difference between the two metals. It is known from photoemission and x-ray absorption studies that changes in surface structure induce subtle, and yet significant, changes in the electronic structure of the catalyst surface (*20*). Hence, at the core of the structure sensitivity issue is the profound influence microscopic surface geometry has on surface electronic structure, and the continued study of this important effect is of great interest in the heterogeneous activation of saturated hydrocarbons.

## REFERENCES AND NOTES

1. J. H. Sinfelt, *Bimetallic Catalysts: Discoveries, Concepts, and Applications* (Wiley, New York, 1983), pp. 130–157.
2. A. E. Shilov, *Activation of Saturated Hydrocarbons by Transition Metal Complexes* (Reidel, Dordrecht, Netherlands, 1984); R. H. Crabtree, *Chem. Rev.* **85**, 245 (1985); B. Meunier and B. Chaudret, Eds., *Perspectives in the Selective Activation of C–H and C–C Bonds in Saturated Hydrocarbons*, vol. CXXX of the NATO Advanced Study Institutes Series (Reidel, Dordrecht, Netherlands, 1987).
3. D. F. McMillen and D. M. Golden, *Annu. Rev. Phys. Chem.* **33**, 493 (1982).
4. J. C. Rasser, *Platinum-Iridium Reforming Catalysts* (Delft Univ. Press, Delft, Netherlands, 1977), pp. 156–193.
5. M. A. Van Hove, W. H. Weinberg, C.-M. Chan, *Low-Energy Electron Diffraction: Experiment, Theory, and Surface Structure Determination* (Springer-Verlag, Heidelberg, Germany, 1986), pp. 265–272.
6. T. S. Wittrig, P. D. Szuromi, W. H. Weinberg, *J. Chem. Phys.* **76**, 3305 (1982); P. D. Szuromi, J. R. Engstrom, W. H. Weinberg, *ibid.* **80**, 508 (1984).
7. P. D. Szuromi, J. R. Engstrom, W. H. Weinberg, *J. Phys. Chem.* **89**, 2497 (1985).
8. L. E. Firment and G. A. Somorjai, *J. Chem. Phys.* **66**, 2901 (1977).
9. J. A. Rodriquez and D. W. Goodman, *J. Phys. Chem.* **94**, 5342 (1990).
10. Y.-K. Sun and W. H. Weinberg, *J. Vac. Sci. Technol. A* **8**, 2445 (1990).
11. C. B. Mullins and W. H. Weinberg, *J. Chem. Phys.* **92**, 4508 (1990).
12. J. J. Vajo, W. Tsai, W. H. Weinberg, *Rev. Sci. Instrum.* **56**, 1439 (1985). The Ir(111) crystal was cut, polished, and prepared with standard techniques. The crystal surface was cleaned between experiments by heating to 1000 K for 5 min at an $O_2$ pressure of $5 \times 10^{-8}$ torr flowing through the microreactor, followed by annealing to 1625 K for 1 min to desorb the surface oxygen. Thermal desorption spectra of CO, which were in complete agreement with previously published ones from the clean Ir(111) surface [C. M. Comrie and W. H. Weinberg, *J. Chem. Phys.* **64**, 250 (1976)], were measured frequently to verify the cleanliness of the surface. Furthermore, because kinetic data are known to be extremely sensitive to surface conditions, the high degree of reproducibility of the data presented here indicates the absence of surface contamination. The $^{13}C$-labeled ethane [1,2-di-$^{13}C$]$C_2H_6$, 99 atom % $^{13}C$) was obtained from Icon Services and was introduced into the microreactor from a gas-handling manifold that was pumped by a diffusion pump to a base pressure below $10^{-7}$ torr.
13. Under these experimental conditions the dissociative chemisorption of $C_2H_6$ is irreversible, and no gas-phase carbon-containing products of a surface self-hydrogenolysis reaction are formed. The titration conditions and procedure were selected to ensure the complete oxidation of the surface carbon to $^{13}CO_2$.
14. The measurements of $C_2H_6$ activation at defect sites on our Ir(111) sample have been done separately and will be reported elsewhere (D. F. Johnson and W. H. Weinberg, in preparation).
15. C. T. Rettner, H. E. Pfnur, D. J. Auerbach, *Phys. Rev. Lett.* **54**, 2716 (1985); A. C. Luntz and D. S. Bethune, *J. Chem. Phys.* **90**, 1274 (1989); M. B. Lee, Q. Y. Yang, S. T. Ceyer, *ibid.* **87**, 2724 (1987).
16. W. H. Weinberg, in *Dynamics of Gas-Surface Collisions*, C. T. Rettner and M. N. R. Ashfold, Eds. (Royal Society of Chemistry, Cambridge, 1991), pp. 171–220; G. Ehrlich, in *Chemistry and Physics of Solid Surfaces VII*, R. Vanselow and R. F. Howe, Eds. (Springer-Verlag, Heidelberg, Germany, 1989), pp. 1–64.
17. W. H. Weinberg, in *Kinetics of Interface Reactions*, H. J. Kreuzer and M. Grunze, Eds. (Springer-Verlag, Heidelberg, Germany, 1987), pp. 94–121; W. H. Weinberg, *Langmuir* **9**, 655 (1993).
18. C. T. Campbell, Y.-K. Sun, W. H. Weinberg, *Chem. Phys. Lett.* **179**, 53 (1991).
19. C. T. Rettner, E. K. Schweizer, H. Stein, D. J. Auerbach, *Phys. Rev. Lett.* **61**, 986 (1988).
20. M. Cardona and L. Ley, Eds., *Photoemission in Solids I and II*, vols. XXVI and XXVII of *Topics in Applied Physics* (Springer-Verlag, Heidelberg, Germany, 1978); J. W. Gadzuk, in *Electronic Structure and Reactivity of Metal Surfaces*, vol. XVI of the NATO Advanced Study Institutes, Series B, E. G. Derouane and A. A. Lucas, Eds. (Plenum, New York, 1976), pp. 341–387; J. C. Fuggle and J. E. Inglesfield, Eds., *Unoccupied Electronic States: Fundamentals for XANES, EELS, IPS, and BIS*, vol. LXIX of *Topics in Applied Physics* (Springer-Verlag, Heidelberg, Germany, 1992); J. H. Sinfelt and G. D. Meitzner, *Acc. Chem. Res.* **26**, 1 (1993).
21. This work was supported by the Department of Energy (grant DE-FG03-89ER14048), the Donors of the Petroleum Research Fund administered by the American Chemical Society (grant ACS-PRF-23801-AC5-C), and the Universitywide Energy Research Group of the University of California.

1 March 1993; accepted 27 April 1993

---

# Ecological Roulette: The Global Transport of Nonindigenous Marine Organisms

James T. Carlton and Jonathan B. Geller

**Ocean-going ships carry, as ballast, seawater that is taken on in port and released at subsequent ports of call. Plankton samples from Japanese ballast water released in Oregon contained 367 taxa. Most taxa with a planktonic phase in their life cycle were found in ballast water, as were all major marine habitat and trophic groups. Transport of entire coastal planktonic assemblages across oceanic barriers to similar habitats renders bays, estuaries, and inland waters among the most threatened ecosystems in the world. Presence of taxonomically difficult or inconspicuous taxa in these samples suggests that ballast water invasions are already pervasive.**

Biological invasions are a great threat to the integrity of natural communities of plants and animals and to the preservation of endangered species (*1*). Most invasion studies have focused on terrestrial and freshwater systems in which one or a few successful invaders have had a catastrophic impact on native species (*2*). Island ecosystems, such as New Zealand and the Hawaiian Islands, have in particular been devastated by the invasion of nonindigenous species (*1–3*). Invasions in marine systems have been less studied (*4*), but are of such magnitude that marine invasions may be leading to profound ecological changes in the ocean.

Any mechanism for rapidly transporting large volumes of water containing plankton from shallow, coastal waters across natural oceanic barriers has the potential to facilitate massive invasions of entire assemblages of neritic marine organisms. Such a mechanism exists in the transport of ballast water and plankton by ocean-going ships (*5*), a dispersal mecha-

---

J. T. Carlton, Maritime Studies Program, Williams College, Mystic Seaport, Mystic, CT 06355, and Department of Biology, Williams College, Williamstown, MA 01267.

J. B. Geller, Department of Biological Sciences, University of North Carolina at Wilmington, Wilmington, NC 28403.